JPET Fast Forward. Published on October 10, 2018 as DOI: 10.1124/jpet.118.250936
This article has not been copyedited and formatted. The final version may differ from this version.

Title Page

L-PGDS but not H-PGDS deletion causes hypertension and accelerates thrombogenesis in mice.

Wen-Liang Song, Emanuela Ricciotti, Xue Liang, Tilo Grosser , Gregory R. Grantand Garret A. FitzGerald

Department of Systems Pharmacology and Translational Therapeutics, Perelman School of Medicine, Pennsylvania, PA 19104, USA. (W-L.S, E.R, X.L, T.G, G.A.F)

The Institute for Translational Medicine and Therapeutics, Perelman School of Medicine, University of Pennsylvania, Philadelphia, PA 19104, USA.(W-L.S, E.R, X.L, T.G, G.R.G, G.A.F)

Department of Genetics, University of Pennsylvania, Philadelphia, PA 19104, USA.(G.R.G)

JPET Fast Forward. Published on October 10, 2018 as DOI: 10.1124/jpet.118.250936
This article has not been copyedited and formatted. The final version may differ from this version.

Running title: L-PGDS causes hypertension and accelerates thrombogenesis.

Author for correspondence: Garret A. FitzGerald, Department of Systems Pharmacology and Translational Therapeutics, Perelman School of Medicine, University of Pennsylvania, Translational Research Center, 3400 Civic Center Blvd, Bldg 421, 10th Floor, Room 116, Philadelphia, PA 19104-5158. Phone number: 215-898-1185. Fax number: 215-573- 9135.

E-mail garret@upenn.edu

Number of text pages: 24

Number of tables: 1

Number of figures: 8

Number of references: 39

Number of words in the Abstract: 201

Number of words in the Introduction: 644

Number of words in the Discussion: 781

Abbreviations: Blood pressure (BP), norepinephrine (NE), epinephrine (E), gene ontology (GO), differentially expressed gene (DEG), False Discovery Rate (FDR).

Recommended section assignment: Cardiovascular.

JPET Fast Forward. Published on October 10, 2018 as DOI: 10.1124/jpet.118.250936
This article has not been copyedited and formatted. The final version may differ from this version.

Abstract

Prostaglandin (PG) D_2 is formed by two distinct prostaglandin D synthases (PGDS): lipocalin-type PGDS (L-PGDS), which acts as a PGD_2 producing enzyme and as extracellular lipophilic transporter, and hematopoietic PGDS (H-PGDS), a sigma glutathione-S-transferase.

PGD_2 plays an important role in the maintenance of vascular function; however, the relative contribution of LPGDS and HPGDS dependent formation of PGD_2 in this setting is unknown.

To gain insight into the function played by these distinct PGDSs, we assessed systemic blood pressure (BP) and thrombogenesis in L-Pgds and H-Pgds KO mice. Deletion of L-Pgds depresses urinary PGD_2 metabolite (PGDM) by ~35% while deletion of H-Pgds does so by ~90%. Deletion of L-Pgds, but not H-Pgds, elevates BP and accelerates the thrombogenic occlusive response to a photochemical injury to the carotid artery. HQL-79, an H-PGDS inhibitor, further depresses PGDM in L-Pgds KO mice, but has no effect on BP or on the thrombogenic response. Gene expression profiling reveals that pathways relevant to vascular function are dysregulated in the aorta of L-Pgds KOs. These results indicate that the functional impact of L-Pgds deletion on vascular homeostasis may result from an autocrine effect of L-PGDS dependent PGD_2 on the vasculature and/or the L-PGDS function as lipophilic carrier protein.

JPET Fast Forward. Published on October 10, 2018 as DOI: 10.1124/jpet.118.250936
This article has not been copyedited and formatted. The final version may differ from this version.

Introduction

Prostaglandin (PG) D_2 is synthesized in both the central nervous system (CNS) and the peripheral tissues (Ricciotti and FitzGerald, 2011). In the brain, PGD_2 is involved in the regulation of sleep and other neurological activities, including pain perception (Ricciotti and FitzGerald, 2011). In peripheral tissues, PGD_2 is produced mainly by mast cells and other cells, including platelets, macrophages, and lymphocytes, and there it plays a role in inflammatory and atopic diseases, although it might also exert an array of immunologically mediated anti-inflammatory functions (Ricciotti and FitzGerald, 2011).

PGD_2 is formed by the action of either lipocalin-like PGD synthase (L-PGDS) or hemopoietic PGD synthase (H-PGDS) (Urade Y and Hayaishi O, 2000). L-PGDS, known also as β trace protein, is a member of the lipocalin superfamily, a group of secretory proteins that bind and transport a variety of lipophilic molecules (Herlong JL and Scott TR, 2006). H-PGDS is a sigma class glutathione-S-transferase family member (Urade Y and Eguchi N, 2002). L-PGDS is expressed mainly in the CNS, retina, male and female genital organs, heart and vasculature, whereas H-PGDS is generally localized to the cytosol of immune and inflammatory cells. PGD_2 exerts it biological effects via two G protein-coupled receptors: the prostaglandin D receptor (DP) and the chemoattractant receptor–homologous molecule expressed on Th2 cells (CRTH2) (Hirai H et al., 2003; Kabashima K and Narumiya S, 2003; Sawyer N et al., 2002).

There is increasing evidence that PGDS and PGD_2 play a relevant role in the modulation of the vascular function (Ricciotti and FitzGerald, 2011). PGD_2 mediates vasodilation and increases vascular permeability (Braun M and Schror K, 1992), relaxation of vascular and non-vascular

smooth muscle (Narumiya S and Toda N, 1985; Hall IP, 2000) reduction ocular pressure (Goh Y et al., 1988), inhibition of platelet aggregation (Song WL et al., 2012) and chemotactic recruitment of inflammatory cells (Herlong JL and Scott TR, 2006).

L-PGDS expression is induced by laminar shear stress via activator protein 1 in vascular endothelial cells (Taba Y et al., 2000; Miyagi M et al., 2005) and it is expressed in synthetic smooth muscle cells in the intimal of atherosclerotic lesions and in coronary plaques of arteries with severe stenosis (Eguchi Y et al., 1997; Hirawa N et al., 2002). Patients with stable angina present significantly higher plasma level of L-PGDS in the cardiac vein than in the coronary artery and its concentration in the cardiac vein decreases immediately after angioplasty (Eguchi Y et al., 1997). Human serum L-PGDS level increases with the progression of atherosclerosis and it is an independent predictor of coronary severity (Inoue T, 2008). Moreover, elevated serum L-PGDS levels are associated with the presence of atrial fibrillation in hypertensive patients (Yalcin MU et al., 2016).

More recently it has been reported that serum level of L-PGDS may represent a biomarker of kidney function (White CA et al., 2015) pregnancy-induced hypertension (Duan B et al., 2016) and active lupus nephritis (Brunner HI et al., 2017).

In mice, L-PGDS deletion accelerates atherogenesis and induced glucose intolerance and obesity Ragolia L et al., 2005; Tanaka R et al., 2009). PGD_2 also plays a relevant role in the evolution of vascular inflammation. In the inflamed intima, PGD_2 is partly produced by H-PGDS-producing inflammatory cells that are chemotactically attracted to the vasculature (Herlong JL and Scott TR, 2006). PGD_2 has been shown to inhibit expression of pro-inflammatory genes, such as inducible nitric oxide synthase and plasminogen activator inhibitor-1 in vascular cells (Nagoshi H et al., 1998; Negoro H et al., 2002).

JPET Fast Forward. Published on October 10, 2018 as DOI: 10.1124/jpet.118.250936
This article has not been copyedited and formatted. The final version may differ from this version.

The major objective of the present study was to elucidate the relative contributions of L-PGDS and H-PGDS derived PGD_2 to blood pressure (BP) homeostasis and thrombogenesis in mice. Our results indicate that H-PGDS makes a more substantial contribution than L-PGDS to PGD_2 biosynthesis, as reflected by the major urinary PGD_2 metabolite. Deletion of L-Pgds, but not of H-Pgds, predisposed both to higher BP and increased thrombogenesis.

Material and methods

Animals:

All animal protocols were approved by the University of Pennsylvania Institutional Animal Care and Use Committee. L-Pgds knock-out mice (L-Pgds KO, kindly provided by Dr. Yoshihiro Urade, Osaka, Japan), and H-Pgds knock-out mice (H-Pgds KO, kindly provided by Dr. Yoshihide Kanaoka, Boston, MA), all on a C57/BL6 background. Hence, wild type (WT) littermate controls were used in both sets of studies.

HQL-79, a H-PGDS inhibitor, was purchased from Tocris Bioscience.

WT and L-Pgds KO mice received HQL-79 (30 mg/kg/day in 0.5% methyl cellulose) by oral gavage for 10 days as previously reported (Aritake K et al., 2006; Mohri I et al., 2009).

Peritoneal macrophage culture

Peritoneal macrophages were collected 4 days after intraperitoneal injection of 0.5 mL of 10% thioglycollate (Sigma Chemicals, St Louis, Mo). Non-adherent cells were removed after 2 hours of incubation. Adherent cells were treated with 5 μg/mL of lipopolysaccharide (LPS, Sigma Chemicals, St. Louis, Mo) for 4 and 24 hours.

Mass spectrometric analysis of prostanoids and their metabolites

Prostanoids or their metabolites were measured by mass spectrometry as described previously (Song WL, et al., 2007). Briefly, macrophage production of PGD_2 was determined by quantification of PGD_2 in cell culture supernatants and normalized with total protein content. Systemic production of PGE_2, PGD_2, TxA_2, and prostacyclin (PGI_2) were determined by quantification of their major urinary metabolites (7-hydroxy-5,11-diketotetranorprostane-1,16-dioic acid [PGE-M], 11,15-dioxo-9α-hydroxy-, 2,3,4,5-tetranorprostan-1,20-dioic acid [tetranor PGD-M], 2,3-dinor TxB_2 [Tx-M], and 2,3-dinor 6-keto $PGF_{1\alpha}$ [PGI-M], respectively) in 24-hour collections and normalized with creatinine.

Blood pressure measurement by tail-cuff

Resting systolic blood pressure was measured in conscious WT, L-Pgds KOs and H-Pgds KOs, 8-12 weeks old mice, using a computerized noninvasive tail cuff system (Visitech Systems Inc.). Mice were trained to adapt to the system for 14 days. After that, blood pressure was recorded daily for 3 consecutive days at the same time of the day and in the same way. Data were collected and analyzed using updated BP-2000 software (Visitech Systems Inc.).

Photochemical injury of the carotid artery

L-Pgds KO, H-Pgds KO mice and their littermate WT control mice underwent photochemically induced vascular injury in the carotid artery as previously reported (Cheng Y et al., 2006). Briefly, in anesthetized (sodium pentobarbital, 80 mg/kg) mice 12–16 weeks of age, the left common carotid artery was isolated, and a Doppler flow probe (model 0.5 VB; Transonic Systems Inc.) was applied. The probe was connected to a flowmeter (model T105; Transonic

Systems Inc.) and interpreted with a computerized data acquisition program (PowerLab; AD Instruments). Rose Bengal (Fisher Scientific International) was injected into the jugular vein in a volume of 0.12 ml in a final concentration of 50 mg/kg. Vascular injury was induced by applying 1.5 mW green light laser (540 nm) (Melles Griot) at a distance of 5 cm from the desired site on the carotid artery. Blood flow was monitored for 120 minutes or until stable occlusion occurred. Stable occlusion was defined as a blood flow of 0 ml/min for 3 minutes. Mice that did not occlude within the 120-minute time course were excluded from the experiment. Complete and 50% occlusion time were determined.

Microarray analysis

Thoracic aortas were harvested from male WT and L-Pgds KO mice, 8-12 weeks old. Total RNA was prepared using TRIzol reagent (Invitrogen) and RNeasy columns (Qiagen, Valencia, CA). Samples were prepared in one batch using the Nugen sample preparation protocol and hybridized to Affymetrix MOE430 v2. Data from the CEL files were summarized and normalized using print-tip loess algorithm from the Bioconductor array package for R.6 Patterns of Gene Expression (PaGE) software, which uses the False Discovery Rate (FDR) method, was used to identify statistically significant differentially expressed gene (DEG)s, as previously described (Grant GR et al., 2005). The FDR was set at 10% for all differential gene expression analyses, so that 90% the predicted genes are expected to be true positives. The expression data were clustered (hierarchical method) and visualized using a modified version of the heatmap{stats} function in R.

Ingenuity Pathways Analysis (Ingenuity Systems, www.ingenuity.com) was employed to identify relevant canonical pathways enriched by DEGs between WT and L-Pgds KO mice.

JPET Fast Forward. Published on October 10, 2018 as DOI: 10.1124/jpet.118.250936
This article has not been copyedited and formatted. The final version may differ from this version.

Gene Ontology (GO) enrichment analysis was employed to identify enriched GO biological functions (http://geneontology.org/page/go-enrichment-analysis).

Microarray data are available in the GEO database (http://www.ncbi.nlm.nih.gov/geo/) under accession number GSE77642.

Real-Time PCR analysis

Total RNAs isolated from aortas, brain, adrenal gland and heart (as described above) were reverse-transcribed into cDNA by Taqman Reverse Transcription Reagents (Applied Biosystems, Foster City, CA). TaqMan Gene Expression Assays (Applied Biosystems) for Phenylethanolamine N-methyltransferase (Pnmt, Mm00476993_m1), L-Pgds(Mm01330513_m1), H-Pgds (Mm00479848), Dp1 (Mm00436050_m1) and Dp2 (Mm01223054_m1)were performed on an ABI Prism 7900 Sequence Detection System (Applied Biosystems). Results were normalized with 18s rRNA (Hs99999901_s1).

Statistics

Unless otherwise indicated, between-group comparison was performed using the non-parametric Mann–Whitney test or non-parametric one-way ANOVA. All the comparisons were made between animals of the same age and gender on the same genetic background. A significance threshold of 0.05 was used and it was indicated by a single asterisk. Significance of <0.01 is indicated by double asterisks on the graphs and significance <0.001 is indicated by triple asterisks. All data are presented as mean ± SEM unless otherwise stated.

Results

JPET Fast Forward. Published on October 10, 2018 as DOI: 10.1124/jpet.118.250936
This article has not been copyedited and formatted. The final version may differ from this version.

Differential impact of L-Pgds and H-Pgds deletion on urinary PGD_2 metabolite

Deletion of L-Pgds depressed PGDM by ~30% in both genders when compared to wild type littermate controls (by 34.5% in males, $P < 0.05$, n = 14-15; by 35.3 % in females, $P < 0.05$, n = 11, Fig.1A). Deletion of H-Pgds had a more pronounced effect, depressing urinary PGDM by ~90% (by 91.3% in males, $P < 0.0001$ n = 12; by 87.8% in females, $P < 0.0001$, n = 11-14; Fig. 1B). There was no evidence of systemic re-diversion of the PGH_2 substrate as urinary PGEM, TXM and PGIM were unaltered in both mutants (Suppl. Fig.1).

Deletion of H-Pgds, but not L-Pgds, suppresses PGD_2 biosynthesis by macrophages

H-Pgds was the primary source of PGD_2 formation under basal conditions and after LPS stimulated peritoneal macrophages (Suppl. Fig. 2). PGD_2 production increased after 24 hrs of LPS stimulation (Suppl. Fig. 2A and 2B). Deletion of H-Pgds almost completely suppressed PGD_2 production by macrophages (by 80 % at baseline, $P < 0.0001$, n = 9-15; by 98% at 24 hrs of LPS stimulation, $P < 0.0001$, n = 10-22, Suppl. Fig. 2A). In contrast, deletion of L-Pgds had no impact on PGD_2 production by macrophages (Suppl. Fig. 2B).

Deletion of L-Pgds, but not H-Pgds, elevates blood pressure

Systolic blood pressure was measured by tail-cuff in both male and female L-Pgds and H-Pgds KOs and their littermate controls. L-Pgds deletion caused a statistically significant increase in systolic blood pressure in both females and males (117.5 ± 2.7 *vs.* 126.3 ± 2.5 mmHg in females, $P < 0.05$, n = 9-11; 119.3 ± 2.4 *vs.* 131.2 ± 4.2 mmHg in males, $P < 0.05$, n = 11-18; Fig. 2 A and B). H-Pgds deletion did not cause any change in blood pressure in either gender (116.9 ± 2.8 *vs.*

112.9± 2.8 mmHg in females, n = 10-11; 111.7 ± 5.4 *vs.* 113.2 ± 7.3 mmHg in males, n = 5-8; Fig. 2 C and D).

Deletion of L-Pgds, but not H-Pgds, accelerates the thrombogenic occlusive response to a photochemical injury of the carotid artery

The time to complete common carotid artery occlusion after photochemical injury was reduced by L-Pgds deletion by approximately 45% in females and 30% in males (68.6 ± 7.1 vs. 38.2 ± 7.8 minutes in females, $P < 0.01$, n = 10-11; 59.0 ± 4.0 vs. 41.7 ± 2.7 minutes in males, $P < 0.001$, n = 11-16; Fig. 3 A and B). The time to complete common carotid artery occlusion in either gender was unaltered by H-Pgds deletion (Fig. 3 C and D).

HQL-79, a selective H-PGDS inhibitor, has no effect on blood pressure or thrombogenic response

HQL-79, a selective inhibitor of H-PGDS (Aritake K et al., 2006; Mohri I et al., 2009), caused a further reduction of PGDM level by approximately 30% in L-Pgds KOs (8.9 ± 0.9 *vs.* 6.0 ± 0.7 ng/mg creatinine, WT *vs*. L-Pgds KO+ vehicle, $P < 0.05$, n = 15-17; 6.0 ± 0.7 vs. 4.0 ± 0.6 ng/mg creatinine, L-Pgds KO+vehicle *vs.* L-Pgds KO+HQL-79, $P < 0.05$, n = 17; Fig. 4 A). The additional reduction of PGDM caused by HQL-79 administration in L-Pgds KO mice did not have any effect on blood pressure (123.6 ± 2.4 *vs.* 123.0 ± 2.5 mmHg, L-Pgds KO+vehicle *vs.* L-Pgds KO+HQL-79, n=18; Fig. 4 B) and on the thrombogenic response (71.5 ± 10.8 *vs.* 63.0 ± 6.2 minutes, L-Pgds KO+vehicle *vs.* L-Pgds KO+HQL-79, n=6-9; Fig. 4 C).

L-Pgds deletion causes dysregulation of genes associated with hypertension and thrombosis

To gain insight into potential mechanisms by which L-Pgds deletion contributes to the hypertensive and pro-thrombotic phenotype, the transcriptome of aorta samples from L-Pgds KO was compared to those from WT mice with microarrays. Deletion of L-Pgds have no effects on expression of H-Pgds, PGD_2 receptors Ptgdr (Dp1) and Ptgdr2 (Dp2) (Suppl Fig 3, 4). The analysis revealed a differential gene expression profile in the aorta from L-Pgds KO compared to control mice. In particular, a total of 454 probes (corresponding to 391 unique genes) were differentially expressed in the aorta of L-Pgds KO mice (q<0.1; Table 1), of which 186 were up-regulated and 268 down-regulated as compared to WTs (Fig. 5). As expected, the samples clustered according to their genotype and the most down-regulated gene in the aorta of L-Pgds KO mice was Ptgds (fold change of 40), which encodes the L-Pgds enzyme.

Among the genes up-regulated in L-Pgds KO mice, we identified Pnmt (fold change of 1.5), a N-methyltransferase that methylates norepinephrine (NE) to form epinephrine (E). We confirmed an increased expression of Pnmt in the aorta, brain and adrenal gland but not in the heart of L-Pgds KO mice by rt-PCR (Fig. 6). Pnmt`s mRNA level was reported to be positively correlated with systemic blood pressure (Reja V et al., 2002) and, indeed both male and females L-Pgds KO showed an increased systolic blood pressure (Fig. 2 A-B).

It has been reported that L-Pgds KO mice show features of the metabolic syndrome that correlates with hypothalamic-pituitary-adrenal (HPA) hyperactivity (Evans JF et al., 2013). Indeed, corticotropin releasing hormone receptor 2 (Crhr2) was upregulated 1.6 fold in the aorta of L-Pgds KO mice.

In addition, significant changes in the expression of a number of genes involved in glucose metabolism and insulin signaling were identified in the aorta of L-Pgds KO mice, including the up-regulation of nicotamide nucleotide transhydrogenase (Nnt, fold change of 2.5) and the down-

JPET Fast Forward. Published on October 10, 2018 as DOI: 10.1124/jpet.118.250936
This article has not been copyedited and formatted. The final version may differ from this version.

regulation of insulin receptor (Insr, fold change of 1.5), insulin degrading enzyme (Ide, fold change 1.4), lipin 1 (Lpin1, fold change of 1.6), Acyl-CoA synthetase medium-chain family member 3 (Acsm3, fold change of 1.6), acyl-CoA synthetase long-chain family member 4 (Acsl4, fold change of 1.8) and glycogen synthase-1 (Gys1, fold change of 1.3).

Changes in the expression of these genes are consistent with the insulin resistant phenotype observed in the L-Pgds KO (Ragolia L et al., 2005).

It is well established that insulin resistance contributes to endothelial dysfunction and a consequent predisposition to thrombosis in diabetics. Increased oxidative stress may also contribute to this phenotype (Ceriello A and Motz E, 2004). Indeed, several aortic genes related to the oxidative stress response, such as heme oxygenase 1 (Hmox1, fold change of 1.4), glutathione S-transferase mu (Gstm2, fold change of 1.2) and thioredoxin interacting protein (Txnip, fold change of 1.5) were dysregulated in L-Pgds KO mice.

Finally, Ingenuity Pathways analysis revealed that the top canonical pathways enriched by genes differentially regulated between WT and L-Pgds KO mice are related to the cellular stress response like “Protein Ubiquitination Pathway”, “Unfolded protein response”, “NRF2 mediated oxidative stress response” and “Production of nitric Oxide and reactive oxygen species” (Fig. 7).

Interestingly, GO Enrichment Analysis revealed that all the top10 molecular functions enriched by genes differentially regulated between WT and L-Pgds KO mice are related to protein binding function (Fig. 8) and about 6% of DEGs are transporters and most of them are members of the solute carrier group of membrane transport proteins (solute carrier family 4, 7, 11, 12, 22, 25, 26, 39, 43, 50, Table 1).

Gene expression profiles of L-Pgds and H-Pgds are summarized in Suppl. Table 1

Discussion

JPET Fast Forward. Published on October 10, 2018 as DOI: 10.1124/jpet.118.250936
This article has not been copyedited and formatted. The final version may differ from this version.

Both human and mouse studies indicate an important role of PGD_2 in the vasculature.

In this study, we demonstrated that the systemic biosynthesis of PGD_2 is generated mainly through H-Pgds (about 90%) and only partially through L-Pgds (Fig 1). However, deletion of L-Pgds, but not H-Pgds, elevated systemic blood pressure (Fig. 2) and accelerated the thrombogenic occlusive response to a photochemical injury to the carotid artery in mice (Fig 3). Thus, the effect of L-Pgds deletion on these cardiovascular phenotypes was not directly or quantitatively related to the suppression of systemic PGD_2 biosynthesis. In fact, HQL-79, an H-PGDS inhibitor, further depresses urinary PGDM in L-Pgds KO mice, but has no incremental effect on blood pressure level or the thrombogenic response in mice (Fig 4). Thus, although it is known that PGD_2 can induce relaxation of vascular and non-vascular smooth muscle cells (Braun M and Schror K, 1992; Narumiya S and Toda N, 1985) and inhibit platelet activation and aggregation by increasing adenylate cyclase activity (Bushfield M et al., 1985) we failed to observe any effect of H-Pgds deletion, the major contributor of systemic production of PGD_2, on blood pressure or thrombosis.

Previously, L-PGDS had been linked to blood pressure homeostasis: both serum and urinary levels of L-PGDS are much higher in patients with hypertension than those in normotensive subjects (Hirawa N et al., 2002). Moreover, increased platelet P-selectin expression, an index of platelet activation, is negatively correlated with a decrease in serum L-PGDS after percutaneous transluminal coronary angioplasty in the coronary sinus (Inoue T et al., 2001).

L-PGDS, a member of the lipocalin superfamily, functions as a PGD_2-producing enzyme and as a lipophilic carrier protein in the extracellular environment, binding several molecules, such as retinoids, thyroid hormones, bile pigments, fatty acids, hemoglobin and cannabinoid metabolites (Herlong JL and Scott TR, 2006; Orenes-Piñero E et al., 2013, Elmes MW et al., 2018; Zhou Y

et al., 2010). Recently, it has also been reported that L-PGDS can bind hydrophilic ligands like NADPH (Qin S et al., 2015).

The role of L-PGDS as lipophilic carrier protein has already been linked to the insulin resistant and atherosclerotic phenotypes observed in L-Pgds KO mice (Ragolia L et al., 2005).

The role of L-PGDS as a retinoid transporter might be involved in this process since a link exists between the retinoid X receptor and adipogenesis (Ragolia L et al., 2005).

Here, an unbiased analysis of the aortic transcriptomic profile revealed that genes relevant to blood pressure and thrombosis are dysregulated in L-Pgds KO mice compared to the controls (Table 1). Pnmt was one of genes most highly over expressed in the aorta (and other tissues relevant to catecholamine biosynthesis, such as brain and adrenal glands) of L-Pgds deficient mice (Fig 6).

Previously, it has been reported that deletion of L-Pgds accelerates glucose intolerance and insulin resistance (Ragolia L et al., 2005). Indeed, several genes involved in glucose metabolism and insulin signaling were differentially regulated in the aorta of L-Pgds KO mice compared to wild type mice, including up-regulation of Nnt and down-regulation of Insr, Lipin 1, Acsm3, Acsl4 and Gys1. Moreover, Ingenuity Pathway Analysis revealed that pathways related to cellular stress response like “Protein Ubiquitination Pathway”, “Unfolded protein response”, “NRF2 mediated oxidative stress response” and “Production of nitric Oxide and reactive oxygen species” were enriched in those genes differentially expressed in WT and L-Pgds KO mice. These data are consistent with the hypothesis that insulin resistance in L-Pgds KO mice might result in oxidative stress in the vasculature, resulting in the hypertension and exaggerated thrombogenesis that we observed.

JPET Fast Forward. Published on October 10, 2018 as DOI: 10.1124/jpet.118.250936
This article has not been copyedited and formatted. The final version may differ from this version.

Although suppression of PGD_2 biosynthesis by deletion of H-Pgds has no resultant cardiovascular phenotype, this might be expected given the absence of expression of its transcript in vascular cells. While the phenotypes consequent to deletion of L-Pgds may reflect its actions independent of PGD_2, it is possible that L-Pgds confers PGD_2 dependent cardioprotection via an autocrine effect in the vasculature. Off target effects, particularly mediated via its transporter function, may also confer cardioprotection, alone or in conjunction with an impact on PGD_2. Indeed, 6% of the 391 unique genes differentially expressed in the aorta of L-Pgds deficient mice compared to control mice are transporters and most of them are members of the solute carrier group of membrane transport proteins (Fig. 9, Table 1). Moreover, the GO Enrichment Analysis revealed that all the top molecular functions enriched by genes differentially regulated between WT and L-Pgds KO mice are related to binding functions (Fig. 8).

In conclusion, these results indicate that the functional impact of L-Pgds deletion on vascular homeostasis may result from an autocrine effect of L-PGDS dependent PGD_2 on the vasculature and/or the L-PGDS function as lipophilic carrier protein.

Acknowledgments

We thank Nicholas Lahens, Helen Zou, Wenxuan Li, Weili Yan and Faith Coldren for technical help and advice.

Authorship Contributions

Participated in research design: Song, Ricciotti, FitzGerald.

Conducted experiments: Song, Ricciotti, Liang.

JPET Fast Forward. Published on October 10, 2018 as DOI: 10.1124/jpet.118.250936
This article has not been copyedited and formatted. The final version may differ from this version.

Contributed new reagents or analytic tools: Song, Ricciotti.

Performed data analysis: Song, Ricciotti, Grosser, Grant.

Wrote or contributed to the writing of the manuscript: Song, Ricciotti, FitzGerald.

References

Aritake K, Kado Y, Inoue T, Miyano M, Urade Y (2006) Structural and functional characterization of HQL-79, an orally selective inhibitor of human hematopoietic prostaglandin D synthase. J Biol Chem 281:15277-15286.

Braun M and Schror K (1992) Prostaglandin D2 relaxes bovine coronary arteries by endothelium-dependent nitric oxide-mediated cGMP formation. Circ Res 71:1305–1313.

Brunner HI, Bennett MR, Gulati G, Abulaban K, Klein-Gitelman MS, Ardoin SP, Tucker LB, Rouster-Stevens KA, Witte D, Ying J, Devarajan P (2017) Urine Biomarkers to Predict Response to Lupus Nephritis Therapy in Children and Young Adults. J Rheumatol 44:1239-1248.

Bushfield M, McNicol A, MacIntyre DE (1985) Inhibition of platelet-activating-factor-induced human platelet activation by prostaglandin D2. Differential sensitivity of platelet transduction processes and functional responses to inhibition by cyclic AMP. Biochem J 232:267-271.

Ceriello A, Motz E (2004) Is oxidative stress the pathogenic mechanism underlying insulin resistance, diabetes, and cardiovascular disease? The common soil hypothesis revisited. Arterioscler Thromb Vasc Biol 24:816-823.

Cheng Y, Wang M, Yu Y, Lawson J, Funk CD, Fitzgerald GA (2006) Cyclooxygenases, microsomal prostaglandin E synthase-1, and cardiovascular function. J Clin Invest 116:1391-1399.

Duan B, Zhang L, Ding X, Li L, Li Y, Geng H, Ma Y (2016) Serum Beta-Trace Protein as a Novel Predictor of Pregnancy-Induced Hypertension. J Clin Hypertens (Greenwich) 18:1022-1026.

Eguchi Y, Eguchi N, Oda H, Seiki K, Kijima Y, Matsu-ura Y, Urade Y, Hayaishi O (1997) Expression of lipocalin-type prostaglandin D synthase (β-trace) in human heart and its accumulation in the coronary circulation of angina patients. Proc Natl Acad Sci USA 94:14689–14694.

Elmes MW, Volpe AD, d'Oelsnitz S, Sweeney JM, Kaczocha M (2018) Lipocalin-Type Prostaglandin D Synthase Is a Novel Phytocannabinoid-Binding Protein. Lipids 53:353-360.

Evans JF, Islam S, Urade Y, Eguchi N, Ragolia L (2013) The lipocalin-type prostaglandin D2 synthase knockout mouse model of insulin resistance and obesity demonstrates early hypothalamic-pituitary-adrenal axis hyperactivity. J Endocrinol 216:169-180.

Goh Y, Nakajima M, Azuma I, Hayaishi O (1988) Br. J. Ophthalmology 72:461–464.

Grant GR, Liu J, Stoeckert CJ, Jr (2005) A practical false discovery rate approach to identifying patterns of differential expression in microarray data. Bioinformatics 21:2684-2690.

Hall IP (2000) Second messengers, ion channels and pharmacology of airway smooth muscle. Eur Respir J 15:1120–1117.

Herlong JL and Scott TR (2006) Immunology Letters 102:121-131.

Hirai H, Abe H, Tanaka K, Takatsu K, Sugamura K, Nakamura M, Nagata K (2003) Gene structure and functional properties of mouse CRTH2, a prostaglandin D2 receptor. Biochem Biophys Res Commun 307:797–802.

Hirawa N, Uehara Y, Yamakado M, Toya Y, Gomi T, Ikeda T, Eguchi Y, Takagi M, Oda H, Seiki K, Urade Y, Umemura S (2002) Lipocalin-type prostaglandin d synthase in essential hypertension. Hypertension 39:449–454.

Inoue T, Eguchi Y, Matsumoto T, Kijima Y, Kato Y, Ozaki Y, Waseda K, Oda H, Seiki K, Node K, Urade Y (2008) Lipocalin-type prostaglandin D synthase is a powerful biomarker for severity of stable coronary artery disease. Atherosclerosis 201:385-391.

Inoue T, Takayanagi K, Morooka S, Uehara Y, Oda H, Seiki K, Nakajima H, Urade Y (2001) Serum prostaglandin D synthase level after coronary angioplasty may predict occurrence of restenosis. Thromb Haemost. 85:165-170.

Kabashima K and Narumiya S (2003) The DP receptor, allergic inflammation and asthma. Prostaglandins Leukot Essent Fatty Acids 69:187–194.

Miyagi M, Miwa Y, Takahashi-Yanaga F, Morimoto S, Sasaguri T (2005) Activator protein-1 mediates shear stress-induced prostaglandin d synthase gene expression in vascular endothelial cells, Arterioscler. Thromb. Vasc. Biol 25:970–975.

Mohri I, Aritake K, Taniguchi H, Sato Y, Kamauchi S, Nagata N, Maruyama T, Taniike M, Urade Y (2009) Inhibition of prostaglandin D synthase suppresses muscular necrosis. Am J Pathol 174:1735-1744.

Nagoshi H, Uehara Y, Kanai F, Maeda S, Ogura T, Goto A, Toyo-oka T, Esumi H, Shimizu T, Omata M (1998) Prostaglandin D2 inhibits inducible nitric oxide synthase expression in rat vascular smooth muscle cells. Circ Res 82:204–209.

Narumiya S and Toda N (1985) Different responsiveness of prostaglandin D2-sensitive systems to prostaglandin D2 and its analogues. Br J Pharmacol 85:367–375.

Negoro H, Soo Shin W, Hakamada-Taguchi R, Eguchi N, Urade Y, Goto A, Toyo-Oka T, Fujita T, Omata M, Uehara Y (2002) Endogenous prostaglandin D2 synthesis reduces an increase in plasminogen activator inhibitor-1 following interleukin stimulation in bovine endothelial cells. J Hypertens 20:1347–1354.

Orenes-Piñero E, Manzano-Fernández S, López-Cuenca Á, Marín F, Valdés M, Januzzi JL (2013) β-Trace protein: from GFR marker to cardiovascular risk predictor. Clin J Am Soc Nephrol 8:873-881.

Qin S, Shimamoto S, Maruno T, Kobayashi Y, Kawahara K, Yoshida T, Ohkubo T (2015) Thermodynamic and NMR analyses of NADPH binding to lipocalin-type prostaglandin D synthase. Biochem Biophys Res Commun 468:234-239.

Ragolia L, Palaia T, Hall CE, Maesaka JK, Eguchi N, Urade Y (2005) Accelerated glucose intolerance, nephropathy, and atherosclerosis in prostaglandin D2 synthase knock-out mice. J Biol Chem 280:29946-19955.

Reja V, Goodchild AK, Pilowsky PM (2002) Catecholamine-related gene expression correlates with blood pressures in SHR. Hypertension 40:342-347.

Ricciotti E and FitzGerald GA (2011) Prostaglandins and inflammation. Arterioscler Thromb Vasc Biol 31:986-1000.

Sawyer N, Cauchon E, Chateauneuf A, Cruz RP, Nicholson DW, Metters KM, O'Neill GP, Gervais FG (2002) Molecular pharmacology of the human prostaglandin D2 receptor, CRTH2. Br J Pharmacol 137:1163–1172.

Song WL, Lawson JA, Wang M, Zou H, FitzGerald GA (2007) Noninvasive assessment of the role of cyclooxygenases in cardiovascular health: a detailed HPLC/MS/MS method. Methods Enzymol 433:51-72.

Song WL, Stubbe J, Ricciotti E, Alamuddin N, Ibrahim S, Crichton I, Prempeh M, Lawson JA, Wilensky RL, Rasmussen LM, Puré E, FitzGerald GA (2012) Niacin and biosynthesis of PGD_2 by platelet COX-1 in mice and humans. J Clin Invest 122:1459-1468.

Taba Y, Sasaguri T, Miyagi M, Abumiya T, Miwa Y, Ikeda T, Mitsumata M (2000) Fluid shear stress induces lipocalin-type prostaglandin D2 synthase expression in vascular endothelial cells. Circ Res 86:967–973.

Tanaka R, Miwa Y, Mou K, Tomikawa M, Eguchi N, Urade Y, Takahashi-Yanaga F, Morimoto S, Wake N, Sasaguri T (2009) Knockout of the l-pgds gene aggravates obesity and atherosclerosis in mice. Biochem Biophys Res Commun 378:851-856.

Urade Y and Eguchi N (2002) Lipocalin-type and hematopoietic prostaglandin D synthases as a novel example of functional convergence Prostaglandins Other Lipid Mediat 68-69:375-382.

Urade Y and Hayaishi O (2000) Prostaglandin D synthase: structure and function. Vitam Horm 58:89-120.

White CA, Ghazan-Shahi S, Adams MA (2015) β-Trace protein: a marker of GFR and other biological pathways. Am J Kidney Dis 65:131-146.

Yalcin MU, Gurses KM, Kocyigit D, Kesikli SA, Tokgozoglu L, Guc D, Aytemir K, Ozer N (2016) Elevated Serum Beta-Trace Protein Levels are Associated With the Presence of Atrial Fibrillation in Hypertension Patients. Clin Hypertens (Greenwich) 8:439-443.

Zhou Y, Shaw N, Li Y, Zhao Y, Zhang R, Liu ZJ (2010) Structure–function analysis of human l-prostaglandin D synthase bound with fatty acid molecules. FASEB J 24:4668-4677.

Footnotes

JPET Fast Forward. Published on October 10, 2018 as DOI: 10.1124/jpet.118.250936
This article has not been copyedited and formatted. The final version may differ from this version.

This work was supported by National Institutes of Health [Grant HL117798 to Garret A. FitzGerald]. Dr. FitzGerald is the McNeil Professor of Translational Medicine and Therapeutics.

Reprint requests:
Department of Systems Pharmacology and Translational Therapeutics, Perelman School of Medicine, University of Pennsylvania, Translational Research Center, 3400 Civic Center Blvd, Bldg 421, 10th Floor, Room 116, Philadelphia, PA 19104-5158. E-mail garret@upenn.edu

[1] W-L. S. and E.R. should be considered joint first authors

[2] W-L. S., Present address: Vanderbilt University Medicine Center, Cardiology Division Of Department Medicine.

[3] X. L., Present address: Merck Research Laboratories Cambridge Exploratory Science Center, Cambridge, Massachusetts.

JPET Fast Forward. Published on October 10, 2018 as DOI: 10.1124/jpet.118.250936
This article has not been copyedited and formatted. The final version may differ from this version.

Figure Legends

Figure 1. Impact of L-Pgds and H-Pgds deletion on urinary PGD_2 metabolite.

A) Urinary PGD_2 metabolite (PGDM) measured in wild-type (WT) and L-Pgds KO male (blue bars) and female (red bars) mice. B) PGDM measured in WT and H-Pgds KO male (blue bars) and female (red bars) mice. Data in A and B are mean±SEM, n=11-15; *p<0.05; ****p<0.0001.

Figure 2. Effect L-Pgds deletion on systolic blood pressure.

A) Systolic blood pressure (BP) measured in WT and L-Pgds KO female mice. B) BP measured in WT and L-Pgds KO male mice. C) BP measured in WT and H-Pgds KO female mice. D) BP measured in WT and H-Pgds KO male mice. Data are mean±SEM, n=5-18; *p<0.05.

Figure 3. Effect L-Pgds deletion on photochemical induced thrombogenesis in carotid artery.

A) Time to complete common carotid artery occlusion after photochemical injury (Thrombosis time) measured in WT and L-Pgds KO female mice. B) Thrombosis time measured in WT and L-Pgds KO male mice. C) Thrombosis time measured in WT and H-Pgds KO female mice. D) Thrombosis time measured in WT and H-Pgds KO male mice. Data are mean±SEM, n=10-16; **p<0.01.

Figure 4. Effect of HQL-79, a selective H-PGDS inhibitor, on urinary PGD_2 metabolite, systolic blood pressure and thrombogenesis in carotid artery in L-Pgds KO mice.

A) Urinary PGD_2 metabolite (PGDM) measured in wild-type (WT) and in L-Pgds KO male mice treated with vehicle or HQL-79. B) Systolic blood pressure (BP) measured in L-Pgds KO male

mice treated with vehicle or HQL-79. C) Time to complete common carotid artery occlusion after photochemical injury (Thrombosis time) measured in L-Pgds KO male mice treated with vehicle or HQL-79. Data are mean±SEM, n=6-18; *p<0.05; ***p<0.001.

Figure 5. Effect of L-Pgds deletion in mouse aorta.

Heatmap representation of 391 genes differentially expressed (q<0.1) between WT and L-Pgds KO male mice in aorta.

Figure 6. Effect of L-Pgds deletion on Pnmt expression.

Expression of Pnmt in aorta (A), heart (B), brain (C) and adrenal gland (D) in WT and L-Pgds male KO mice measured by rt-pcr. Data are mean±SEM, n=5; *p<0.05.

Figure 7. Ingenuity Pathway Analysis.

Top 20 canonical pathway enriched by genes differentially expressed (q<0.1) between WT and L-Pgds KO mice in aorta.

Figure 8. GO enrichment analysis.

Top 10 GO molecular function enriched by genes differentially expressed (q<0.1) between WT and L-Pgds KO male mice in aorta.

Fig. 1. Impact of L-Pgds and H-Pgds deletion on PGDM

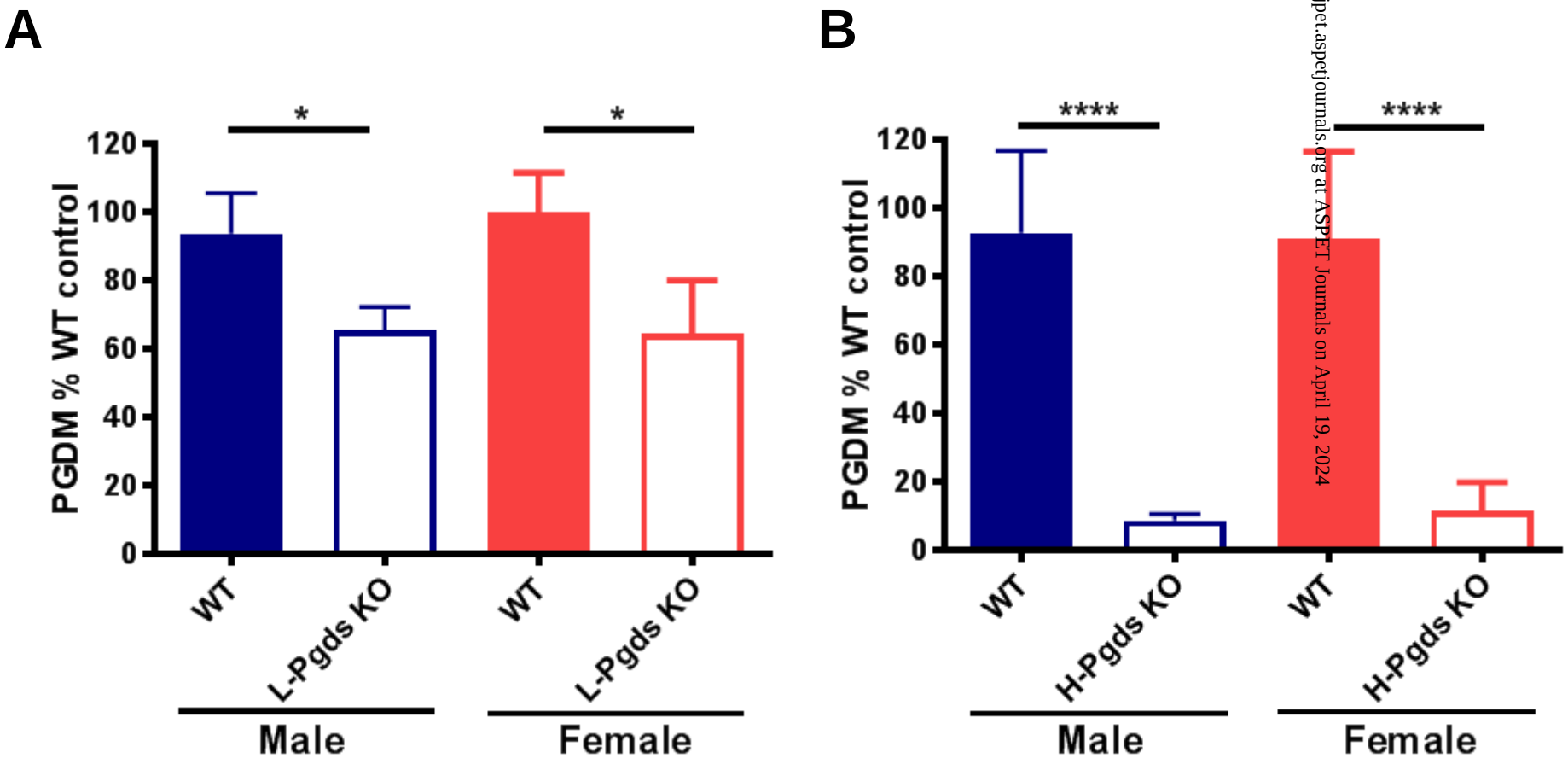

Fig. 2 L-Pgds deletion elevates systolic blood pressure

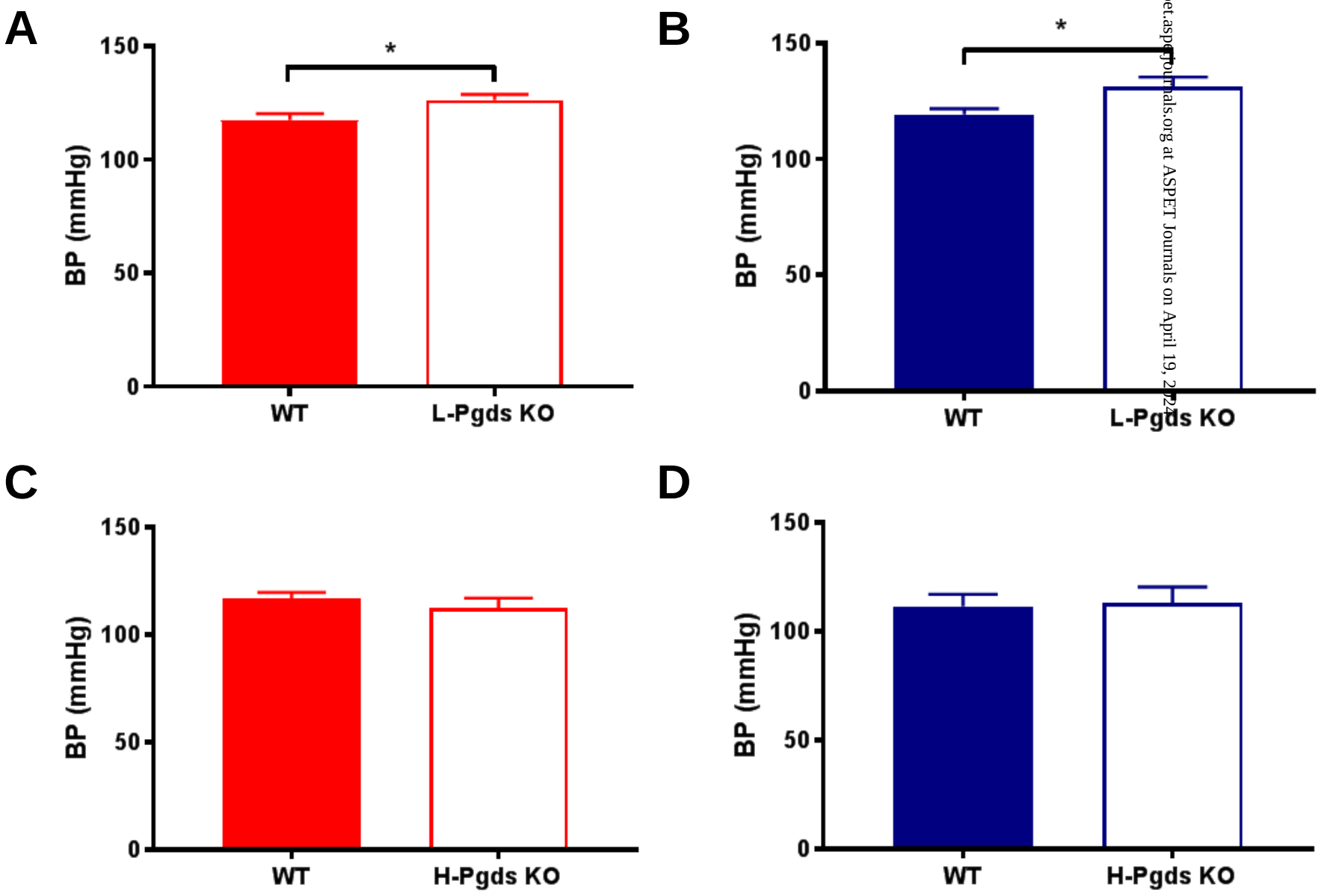

Fig. 3 L-Pgds deletion accelerates photochemical induced thrombogenesis in carotid artery

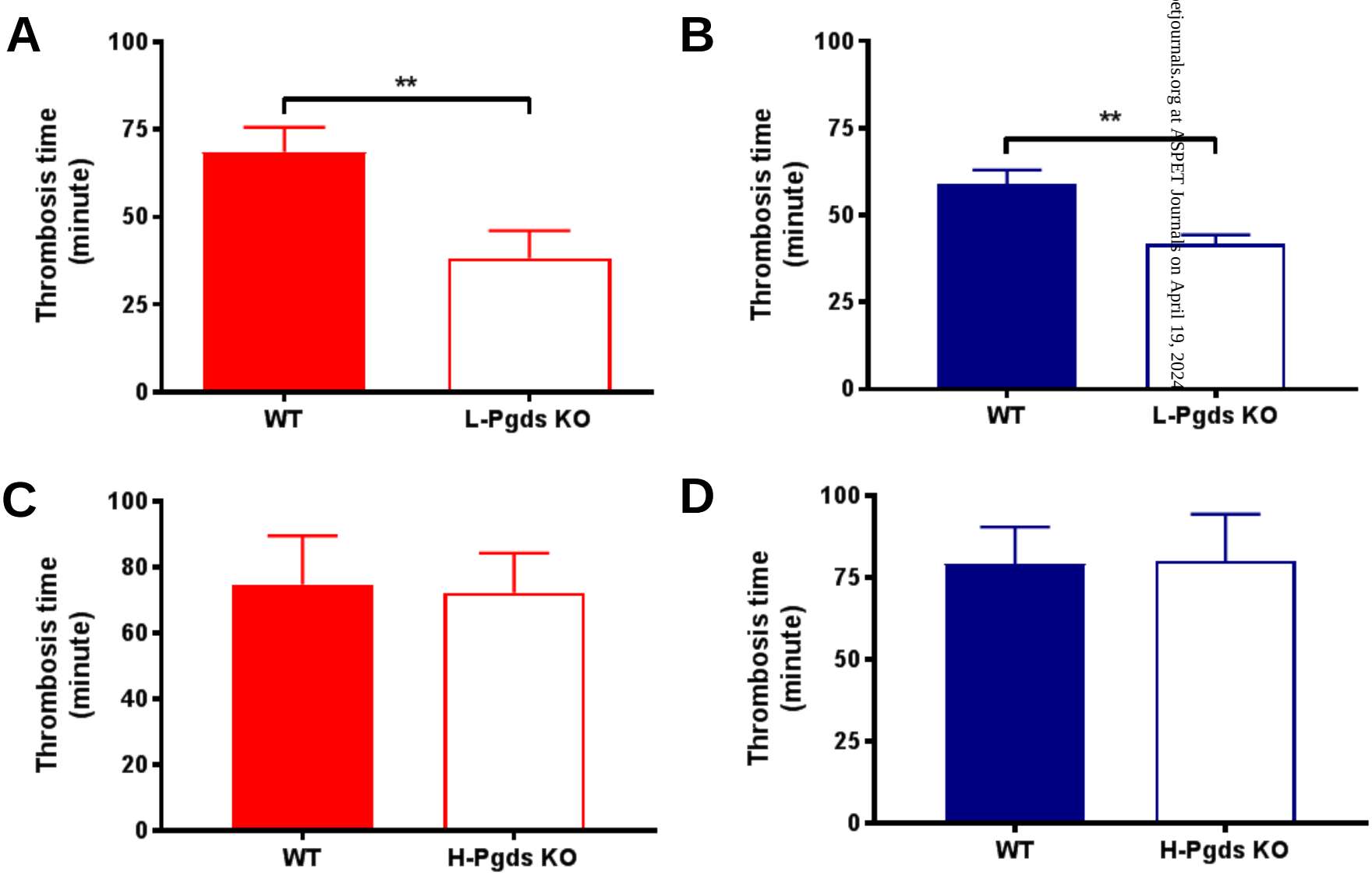

Fig. 4 HQL-79, a H-PGDS inhibitor, does not impact blood pressure and thrombogenic response

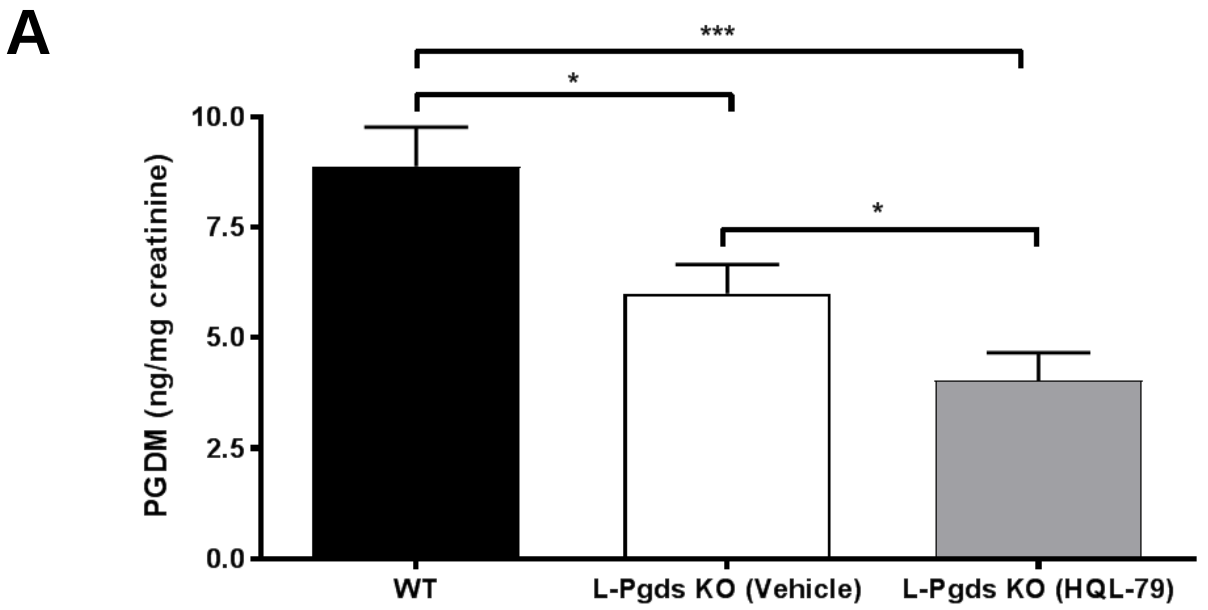

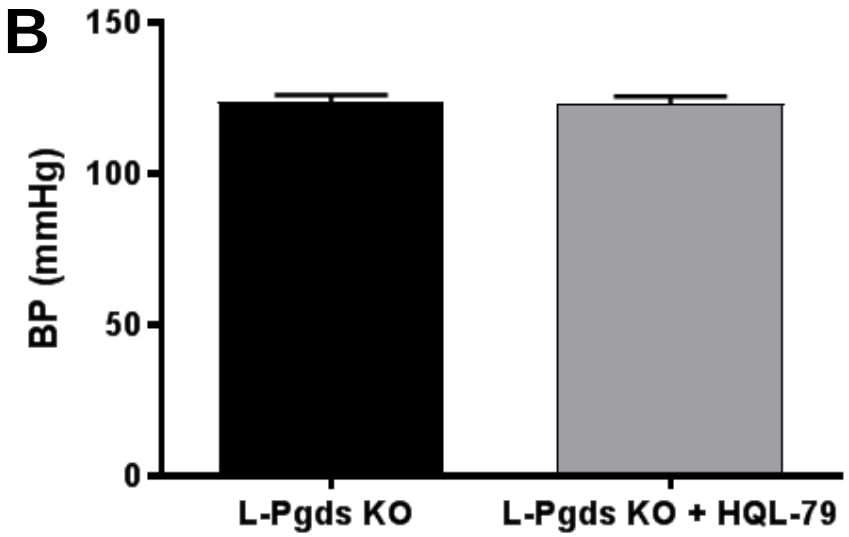

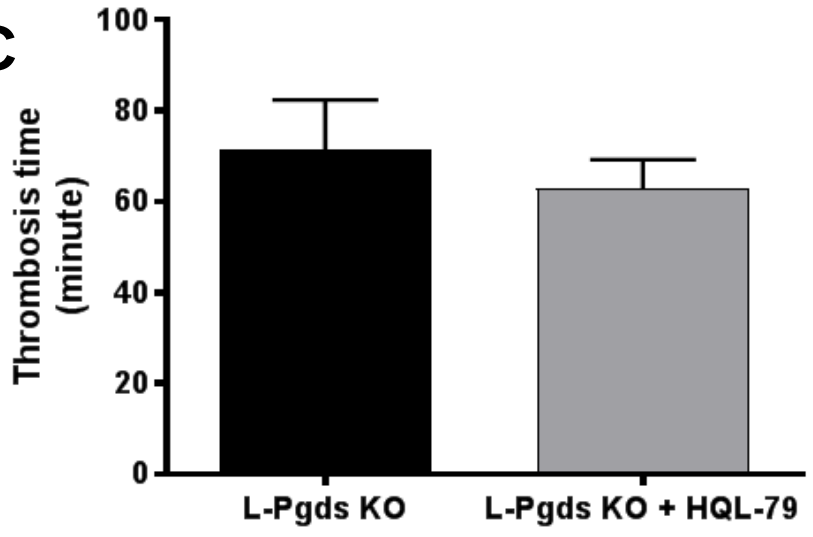

Fig. 5 Effect of L-Pgds deletion in mouse aorta.

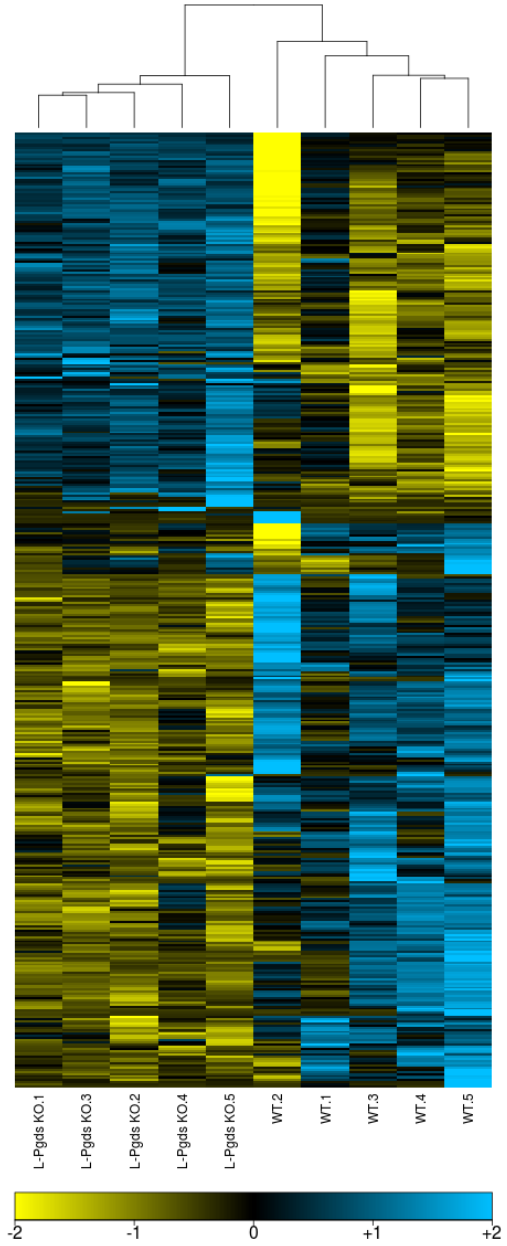

Fig. 6 Effect of L-Pgds deletion on Pnmt expression profile in different tissues

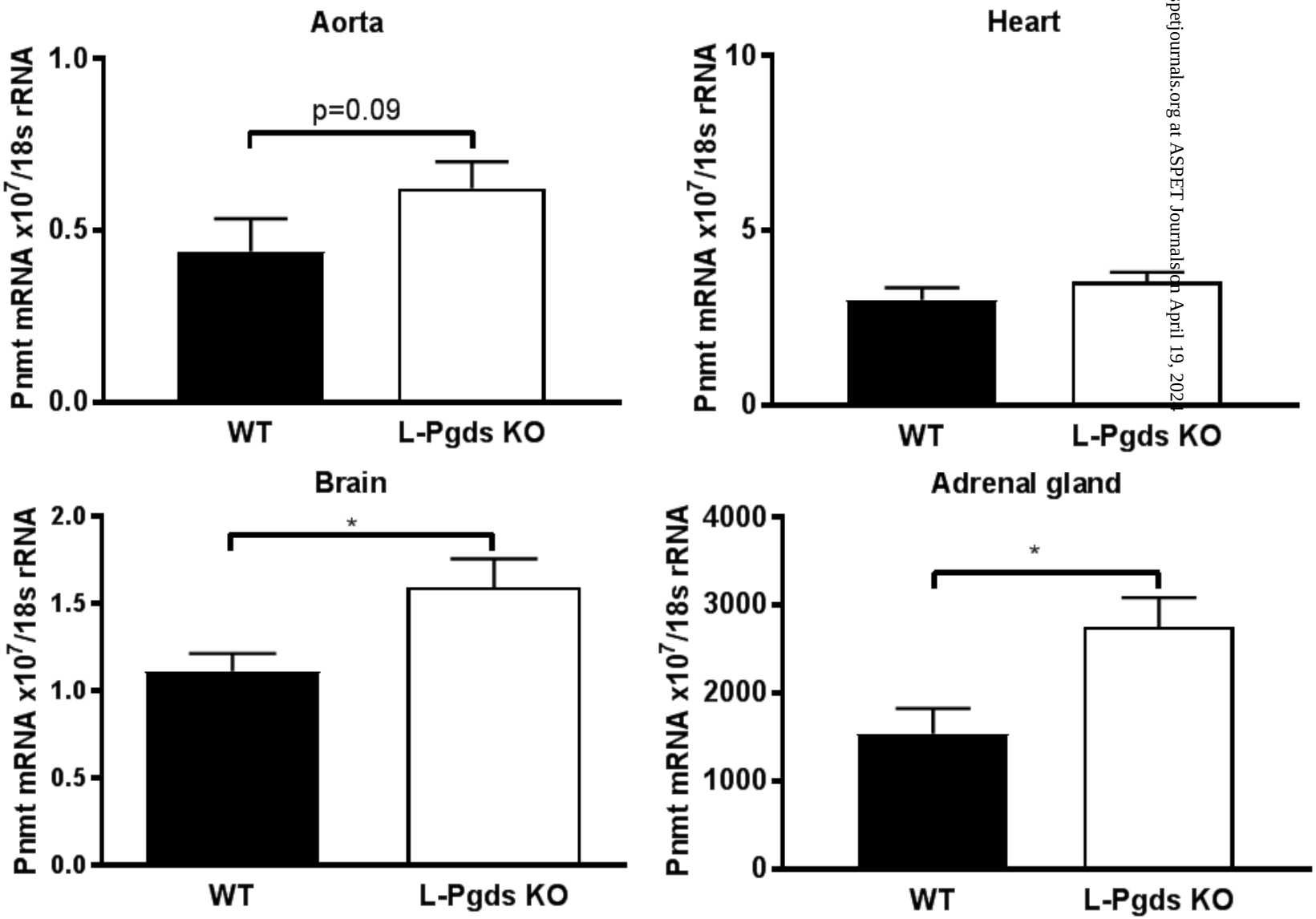

Fig. 7 Top 20 canonical pathway enriched by genes differentially expressed between WT and L-Pgds KO mice

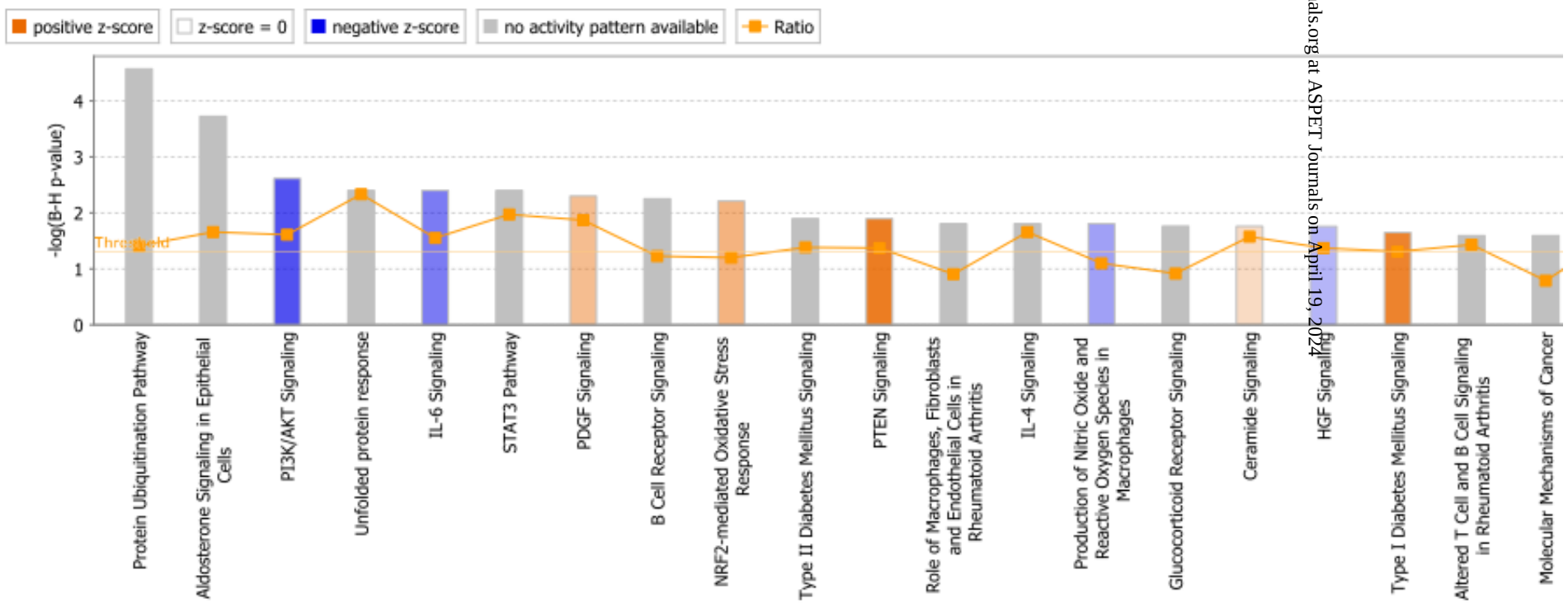

Fig. 8 Top 10 GO molecular function enriched by genes differentially expressed between WT and L-Pgds KO mice

GO molecular function complete	Fold Enrichment	P-value
binding (GO:0005488)	1.54	2.85E-31
protein binding (GO:0005515)	1.87	1.07E-29
heterocyclic compound binding (GO:1901363)	1.78	1.18E-11
organic cyclic compound binding (GO:0097159)	1.76	2.04E-11
enzyme binding (GO:0019899)	2.39	1.10E-08
nucleoside phosphate binding (GO:1901265)	2.18	4.23E-08
nucleotide binding (GO:0000166)	2.18	4.23E-08
carbohydrate derivative binding (GO:0097367)	2.2	4.60E-08
small molecule binding (GO:0036094)	2.04	1.70E-07
receptor binding (GO:0005102)	2.45	2.46E-07

The Journal of Pharmacology and Experimental Therapeutics

L-PGDS but not H-PGDS deletion causes hypertension and accelerates thrombogenesis in mice

Wen-Liang Song, Emanuela Ricciotti, Xue Liang, Tilo Grosser , Gregory R. Grantand Garret A. FitzGerald

SUPPLEMENTARY MATERIAL

Figure Legends

Supplementary Fig. 1: Impact of L-Pgds and H-Pgds deletion on urinary prostanoid metabolites.

A) Urinary TxB_2 metabolite (TxM) measured in wild-type (WT) and L-Pgds KO mice. B) Urinary PGE_2 metabolite (PGEM) measured in WT and L-Pgds KO mice. C) Urinary PGI_2 metabolite (PGIM) measured in WT and L-Pgds KO mice. D) TxM measured in WT and H-Pgds KO mice. E) PGEM measured in WT and H-Pgds KO mice. F) PGIM measured in WT and H-Pgds KO mice. Data are mean±SEM, n=8-17.

Supplementary Fig. 2: Impact of L-Pgds and H-Pgds deletion on PGD_2 biosynthesis in peritoneal macrophages

A) PGD_2 produced at baseline and 24 hrs after lipopolysaccharide (LPS) stimulation by peritoneal macrophages isolated from WT and L-Pgds KO mice. B) PGD_2 produced at baseline and 24 hrs after LPS stimulation by peritoneal macrophages isolated from WT and H-Pgds KO mice. Data are mean±SEM, n=9-22.

Supplementary Fig. 3: Effect of L-Pgds deletion on H-Pgds, Dp1 and Dp2 expression in aorta

Expression of L-pgds (A), H-pgds (B), Dp1 (C) and Dp2 (D) in the aorta of WT and L-Pgds male KO mice obtained by microarray and reported as Fluorescent Intensity converted to log_2 scale. Data are mean±SD, n=5.**Supplementary Fig. 4. Effect of L-Pgds deletion on H-Pgds expression in aorta.**

Expression of L-pgds (A) and H-pgds (B) in the aorta of WT and L-Pgds male KO mice measured by rt-pcr. Data are mean±SD, n=5.

Supplementary Table 1: Gene expression in homo sapiens organisms

Data was extracted from" Expression Atlas - EMBL-EBI". Website: https://www.ebi.ac.uk/gxa/home Gene expression levels were extracted from two representative databases: the 68 FANTOM5 project and the Genotype-Tissue Expression (GTEX project). Expressed levels are categorized as high, medium, low, below cutoff and no data available.

Tissue	H-PGDS (68 FANTOM5)	H-PGDS (GTEX)	L-PGDS (68 FANTOM5)	L-PGDS (GTEX)
Adrenal gland	No data	Low	No data	Medium
Amygdala	Low	Low	low	Medium
Aorta	No data	Low	Below cutoff	Medium
Atrium auricular region	No data	Low	No data	High
Bone morrow	Medium	No data	Low	No data
Breast	Low	Low	Below cutoff	Medium
Brodmann area 24	No data	Low	No data	Medium
Brodmann area 9	No data	Low	No data	Medium
Cervical spinal cord	No data	Low	No data	High
Caudate nucleus	Low	Low	Low	Medium
Cerebellar hemisphere	No data	Below cutoff	No data	Medium
Cerebellum	Low	Below cutoff	Low	Medium
Cerebral cortex	No data	Below cutoff	No data	Medium
Coronary artery	No data	Low	Medium	No data
Colon	Low	No data	Below cutoff	Medium
Diencephalon	Low	No data	Medium	No data
Dorsal thalamus	Low	No data	Low	No data
Dura mater	Low	No data	Low	No data
EBV-transformed lymphocyte	No data	No data	No data	Low
Ectocervix	No data	Low	No data	Medium

Esophagogastric junction	No data	Low	No data	Medium
Esophagus mucosa	No data	Low	No data	Medium
Esophagus mucosa	No data	Low	No data	Medium
Fallopian tube	No data	Low	No data	Medium
Gall bladder	Low	No data	Low	No data
Heart left ventricle	Low	Below cutoff	Low	Medium
Hippocampus proper	No data	Low	No data	Medium
Hypothalamus	No data	Low	No data	Medium
Kidney	Low	No data	Below cutoff	No data
Liver	No data	Below cutoff	No data	Medium
Lower leg skin	No data	Low	No data	Medium
Lung	Low	Low	Low	Medium
Lymph node	Low	No data	Low	No data
Mitral valve	Low	No data	Low	No data
Ovary	Low	Low	Below cutoff	Medium
Pancreas	Low	Below cutoff	Below cutoff	Medium
Penis	Low	No data	Low	No data
Placenta	Low	No data	Below cutoff	Medium
Prostate gland	Low	Low	Low	Medium
Seminal vesicle	Below cutoff	No data	Low	Medium
Smooth muscle tissue	Low	No data	Below cutoff	Medium
Sigmoid colon	No data	Low	No data	Medium
Skeletal muscle tissue	No data	Below cutoff	No data	Medium
Spinal cord	Low	No data	Low	No data
Spleen	Below cutoff	Low	Below cutoff	Medium
Stomach	No data	Low	No data	Medium
Subcutaneous adipose tissue	No data	Low	No data	Medium
Substantia nigra	Low	Low	Medium	High
Suprapubic skin	No data	Low	No data	Medium
Testis	Low	Low	Medium	High
Thyroid gland	No data	Low	No data	Medium
Tibial artery	No data	Low	No data	High
Tongue	Low	No data	Low	No data
Tricuspid valve	Low	No data	Low	Medium
Uterus	Low	Low	Below cutoff	Medium
Vagina	Low	Low	Below cutoff	Medium
Vermiform appendix	Low	Low	Low	No data

Suppl. Fig. 1 No rediversion of PGH_2 substrate to other prostanoids in L-Pgds and in H-Pgds KO mice

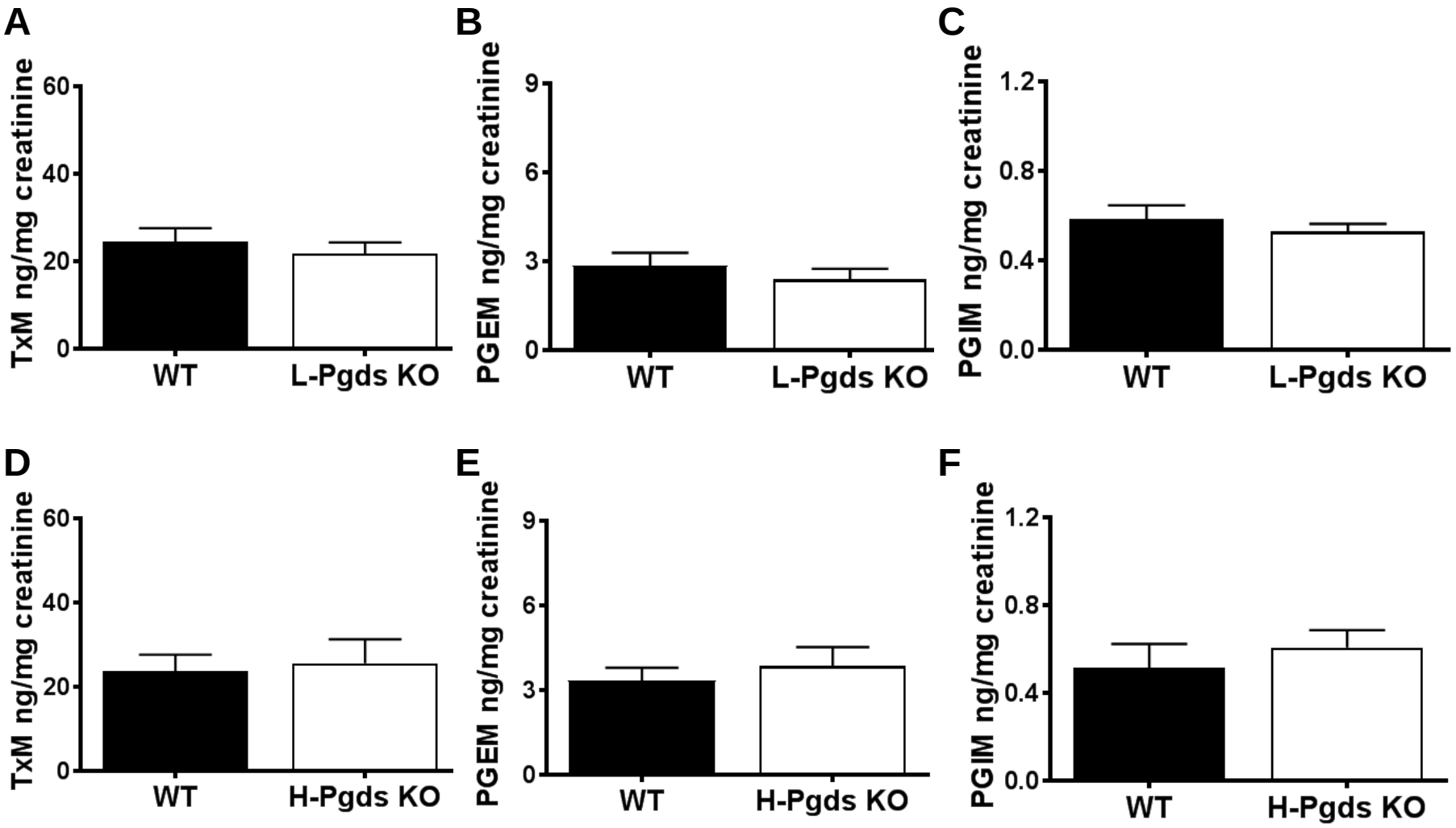

Suppl. Fig. 2 Impact of L-Pgds and H-Pgds deletion on PGD_2 biosynthesis in peritoneal macrophages

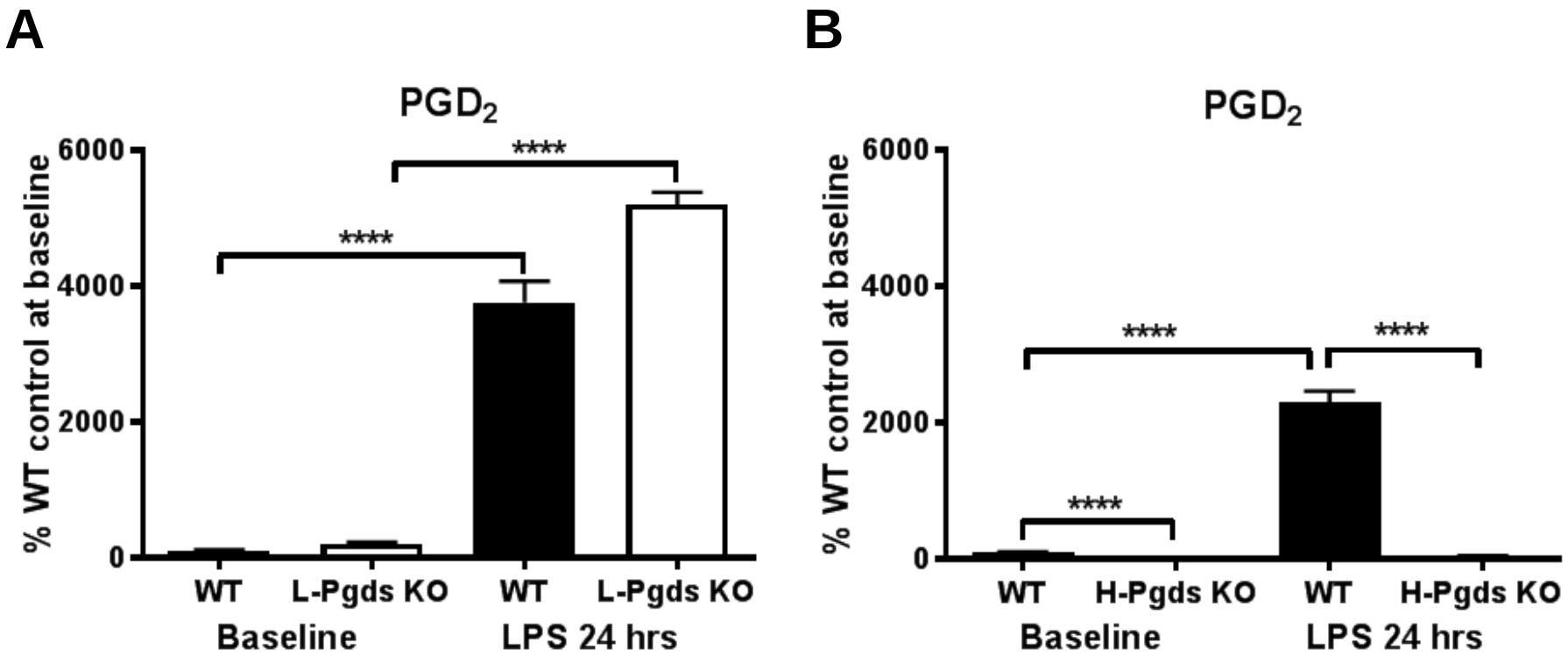

Suppl. Fig. 3 Effect of L-Pgds deletion on H-Pgds, Dp1 and Dp2 expression in aorta

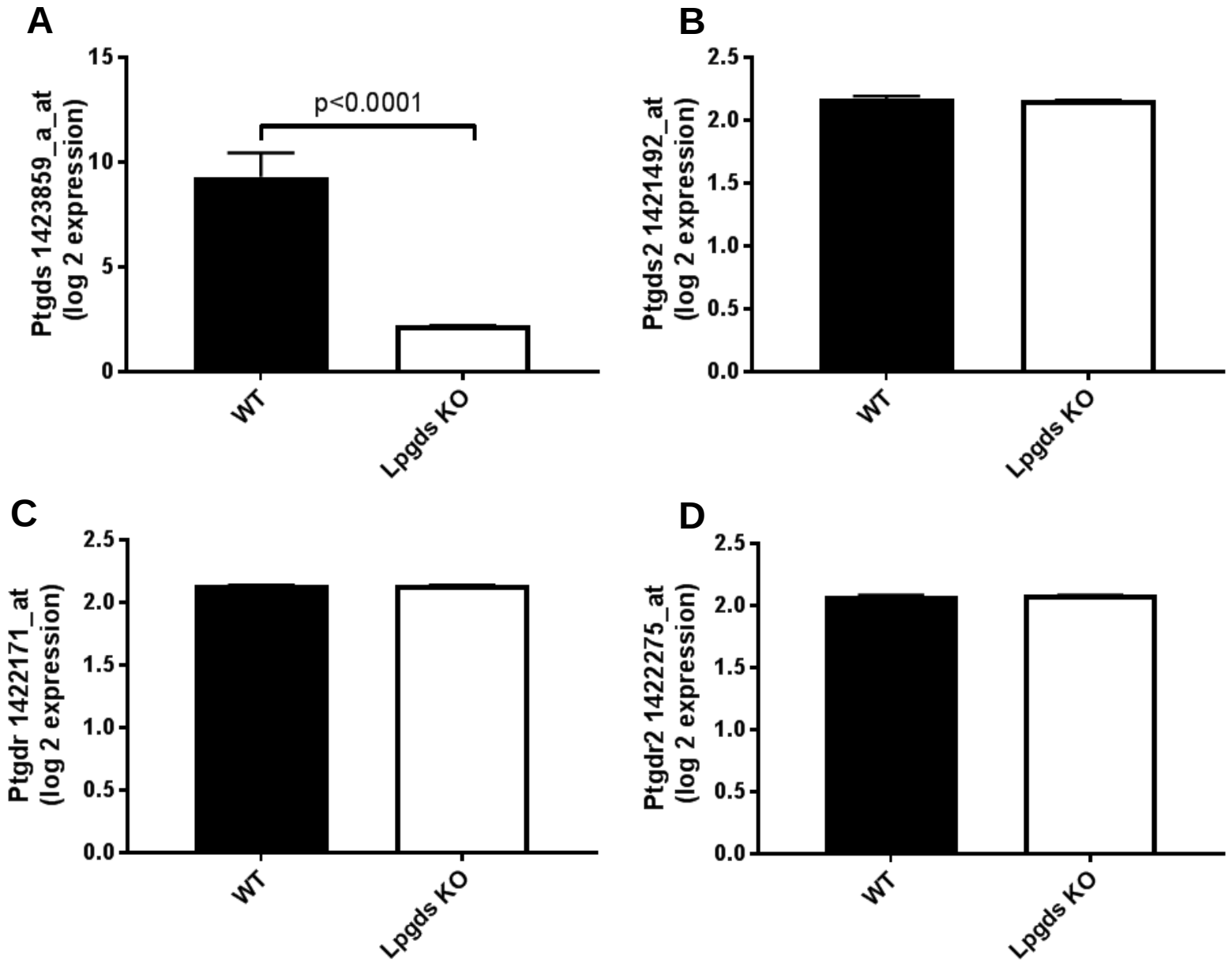

Suppl. Fig. 4 Effect of L-Pgds deletion on H-Pgds expression in aorta